Stability of an Ion Channel in Lipid Bilayers: Implicit Solvent Model Calculations with Gramicidin†

Sharron Bransburg-Zabary, Amit Kessel, Menachem Gutman, and Nir Ben-Tal*

Department of Biochemistry, George S. Wise Faculty of Life Sciences, Tel Aviv University, Ramat Aviv 69978, Israel

Received November 19, 2001

ABSTRACT: Gramicidin is a helical peptide, 15 residues in length, which dimerizes to form ion-conducting channels in lipid bilayers. Here we report calculations of its free energy of transfer from the aqueous phase into bilayers of different widths. The electrostatic and nonpolar contributions to the desolvation free energy were calculated using implicit solvent models, in which gramicidin was described in atomic detail and the hydrocarbon region of the membrane was described as a slab of hydrophobic medium embedded in water. The free energy penalties from the lipid perturbation and membrane deformation effects, and the entropy loss associated with gramicidin immobilization in the bilayer, were estimated from a statistical thermodynamic model of the bilayer. The calculations were carried out using two classes of experimentally observed conformations: a head-to-head dimer of two single-stranded (SS) β-helices and a double-stranded (DS) intertwined double helix. The calculations showed that gramicidin is likely to partition into the bilayer in all of these conformations. However, the SS conformation was found to be significantly more stable than the DS in the bilayer, in agreement with most of the experimental data. We tested numerous transmembrane and surface orientations of gramicidin in bilayers of various widths. Our calculations indicate that the most favorable orientation is transmembrane, which is indeed to be expected from a channel-forming peptide. The calculations demonstrate that gramicidin insertion into the membrane is likely to involve a significant deformation of the bilayer to match the hydrophobic width of the peptide (22 Å), again in good agreement with experimental data. Interestingly, deformation of the bilayer was induced by all of the gramicidin conformations.

The linear gramicidins are a family of small antibiotic peptides that form membrane-spanning ion channels in lipid bilayers (*1*). They form the best characterized ion channels and serve as common models for studying ion conduction through membranes and peptide−membrane interactions (reviewed in refs *2*−*4*). The sequence of the gramicidin A (GA) channel which was used in this study is formyl-L-Val-Gly-L-Ala-D-Leu-L-Ala-D-Val-L-Val-D-Val-L-Trp-D-Leu-L-Trp-D-Leu-L-Trp-D-Leu-L-Trp-ethanolamine (*5*).

The structure of gramicidin A was determined at various conditions (*4*). It has been found that the peptide is very sensitive to the environment and can adapt a variety of conformations. Due to the alternating sequence of L- and D-amino acid residues, the peptide forms β-type helices with a hydrogen-bonding pattern of the backbone similar to that in β-sheets (*6*−*8*). In these β-helices the residues point outward and the carbonyl moieties alternately point upward and downward in the interior of the helix, providing the helices with a hydrophilic pore. The helices may be right- or left-handed; they can differ in the number of residues per turn and, hence, in their dimensions and in the orientation of their chains (*6*, *8*, *9*). Individual molecules can fold into single-stranded helices, which may form head-to-head dimers (*7*, *9*, *10*). Also, double-stranded helices can be formed, in which the two strands run either parallel or antiparallel and which involve intermolecular hydrogen bonding only (*8*).

Over the years, based on accumulative evidence, a consensus has developed that the predominant channel form is a head-to-head dimer of two single-stranded (SS) β-helices (*11*−*15*). Recently, however, with the appearance of a new double-stranded (DS) intertwined structure, this consensus has been challenged (*16*), and there appears to be a controversy as to whether the ion-conducting form is a SS or DS structure (*17*−*20*). To clarify this issue further, we present calculations of the stability of gramicidin in both SS and DS structures in model lipid bilayers.

The length of the hydrophobic core of the gramicidin channel is about 22 Å (*2*, Figure 1), which is significantly shorter than the width of the hydrocarbon region of biological membranes, about 30 Å (*21*). Ample experimental evidence suggests that partitioning of the channel into the bilayer involves local membrane thinning (*2*, *22*−*27*). This local membrane deformation enables the hydrophobic regions on the channel and the membrane to match. Thus, the free energy penalty associated with the transfer of the polar channel ends from water into a nonpolar medium can be avoided.

This argument has been exploited in theoretical models used to provide quantitative interpretation of the experimental data (e.g., refs *28*−*32*). These theoretical models involved

† This work was supported by the Israel Science Foundation (Grant 683/97-1) and Fellowships from the Wolfson and Alon Foundations to N.B.-T.

* To whom correspondence should be addressed. Tel: (972-3) 640-6709. Fax: (972-3) 640-6834. E-mail: bental@ashtoret.tau.ac.il. Website: http://ashtoret.tau.ac.il.

10.1021/bi0120704 CCC: $22.00
Published on Web 05/07/2002

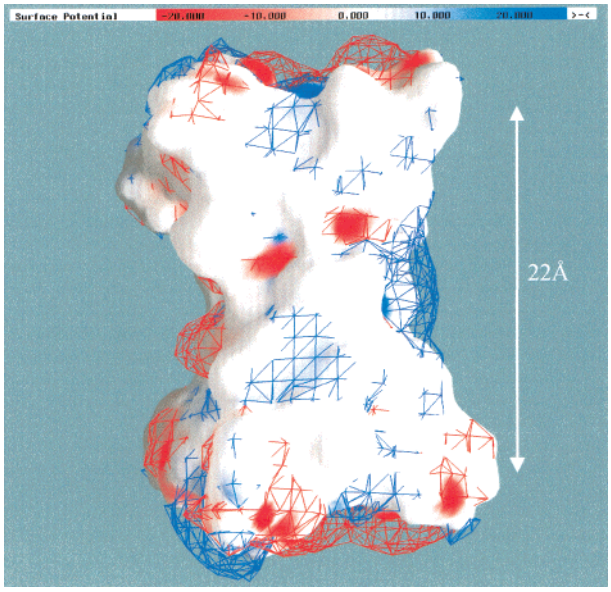

FIGURE 1: Surface electrostatic potential of gramicidin. Gramicidin is in its homodimeric form [the first entry in PDB entry 1GRM (*61*), denoted as 1GRM_1]. The electrostatic potential (ϕ) was color-coded and displayed on the molecular surface of the dimer using GRASP (*91*). Negative potentials (-10 kT/e $< \phi < 0$) are in red, positive potentials ($0 < \phi < 10$ kT/e) are in blue, and neutral potentials are in white. The hydrophobic core of the gramicidin dimer, of ~22 Å length (marked by the arrow), is flanked by the polar C-termini of each monomer. The calculations below show that, in the energetically optimal location, gramicidin is in a transmembrane orientation in the bilayer with the hydrophobic region buried in the hydrocarbon region of the bilayer and the termini protruding into the polar media.

detailed (albeit mean field) treatment of the lipid chains. In contrast, the penalty due to desolvation, which is the driving force for the deformation, was estimated empirically. Despite the crudeness of the models used in the studies, they reproduced the experimental data very well; they have shown that a free energy minimum is obtained when the hydrophobic region of the membrane assumes a width of 22 Å. In contrast, molecular dynamics simulations, which were carried out recently, have suggested that the width of the hydrocarbon region adjacent to the gramicidin channel was more than 22 Å (*33*). Clearly, this issue needs further investigation.

A major theoretical and computational effort has been devoted to understanding the role of gramicidin as an ion-conducting channel (e.g., refs *34*−*36*; reviewed in refs *3*, *37*, and *38*). Moreover, gramicidin is by far the most exhaustively used model in theoretical and computational studies of peptide−membrane interactions (*28*, *31*−*33*, *39*). Nonetheless, the free energy determinants of its partitioning between aqueous solutions and lipid bilayers have never been investigated. In this study, we present detailed continuum solvent calculations of the contribution of desolvation and use these calculations to estimate the free energy of transfer of gramicidin from the aqueous phase into the membrane.

METHODS

The total free energy difference between gramicidin in the membrane and in the aqueous phase (ΔG_{tot}) can be comprised of the sum of the differences in solvation free energy (ΔG_{sol}), peptide conformation (ΔG_{con}), immobilization effects (ΔG_{imm}), membrane perturbation (ΔG_{lip}), and deformation effects (ΔG_{def}) (*40*−*45*; reviewed in refs *21* and *46*):

$$\Delta G_{tot} = \Delta G_{sol} + \Delta G_{con} + \Delta G_{imm} + \Delta G_{lip} + \Delta G_{def} \quad (1)$$

We present here atomic-detailed calculations of the electrostatic (ΔG_{elc}) and nonpolar (ΔG_{np}) contributions to ΔG_{sol}:

$$\Delta G_{sol} = \Delta G_{elc} + \Delta G_{np} \quad (2)$$

ΔG_{sol} is the free energy of transfer of gramicidin from water to a bulk hydrocarbon phase. It accounts for electrostatic contributions resulting from changes in the solvent dielectric constant, as well as for van der Waals and solvent structure effects, which are grouped in the nonpolar term and together define the classical hydrophobic effect. We calculated ΔG_{sol} using the continuum solvent model (*47*−*50*). The method has been described in detail in our earlier studies of the membrane association of helices (*45*, *51*−*53*), monensin−cation complexes (*54*), and small molecules (*55*, *56*). In the following subsections we present a brief outline, with emphasis on the adaptation of the methodology to the gramicidin−membrane system.

Electrostatic Contributions. The calculations were based on a continuum solvent model in which electrostatic contributions were obtained from finite difference solutions to the Poisson−Boltzmann equation (the FDPB method) (*57*). Gramicidin was represented in atomic detail, with atomic radii and partial charges defined at the coordinates of each nucleus. The charges and radii were taken from PARSE, a parameter set that was parametrized to reproduce gas phase-to-water (*58*) and alkane-to-water (*59*) solvation free energies of small organic molecules.

In the FDPB calculations reported here, the boundary between gramicidin and the solvents (water or membrane) was set at the contact surface between the van der Waals surface of the gramicidin molecule and a solvent probe [defined here as having a 1.4 Å radius (*60*)]. Gramicidin and the lipid bilayer were assigned a dielectric constant of 2, and bulk water was assigned a dielectric constant of 80. As for the pore dielectric constant, we tested values between 2 and 80 and concluded that the exact value has very little effect on the free energy of transfer of gramicidin into the bilayer (see Error Estimate below).

The system was mapped onto a lattice of 129^3 grid points, with a resolution of three points per angstrom, and the Poisson equation was numerically solved for the electrostatic potential. The electrostatic free energy was calculated by integration over the potential multiplied by the charge distribution in space.

The Dielectric Constant of the Pore. In all previous implementations (*45*, *51*−*56*), the Poisson equation was solved with two dielectric regions: a high value for water and a low one for the solute (the peptide or protein) and the membrane. We introduced here a third dielectric region (ϵ_{pore}), corresponding to the channel pore. To this end, a cylinder, corresponding approximately to the pore, was defined, its diameter larger than the widest region in the pore, yet smaller than the external region of gramicidin. The height of the cylinder was set to be equal to the hydrophobic length of gramicidin, e.g., 22 Å for the 1GRM structure (*61*). Beyond this region, the channel flares out, and the internal water is less confined. Thus, the value of the solvent was

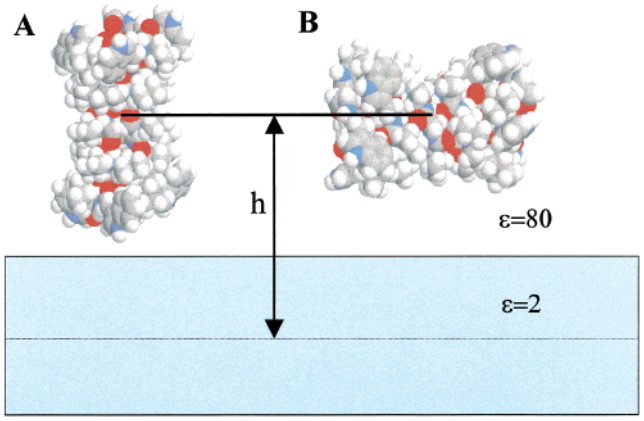

FIGURE 2: Modes of gramicidin insertion. Schematic diagram showing two hypothetical insertion processes of gramicidin into a lipid bilayer: (A) vertical insertion, in which the principal axis of gramicidin is perpendicular to the membrane surface (see also Figure 3); (B) horizontal insertion, in which the principal axis is parallel to the membrane surface (see also Figure 5). The distance *h* is measured between the geometrical center of gramicidin and the bilayer midplane. The gramicidin structure (1GRM_1) is shown as a space-filling model in its homodimeric form, and the hydrocarbon region of the bilayer is depicted by the shaded rectangle. Each gramicidin monomer is a β-helix of disklike shape, and the monomers are noncovalently bound to each other via their N-termini, while their C-termini are solvent exposed. Oxygen atoms are in red, carbon atoms are in gray, nitrogen atoms are in blue, and hydrogen atoms are in white.

assigned. The free space within the cylinder, that is, space that was unoccupied by gramicidin atoms, was considered to be the intrachannel matrix and was assigned the dielectric constant ϵ_{pore}.

Nonpolar Contributions. The nonpolar contribution to the solvation free energy, G_{np}, was assumed to be proportional to the water-accessible surface area of gramicidin, ASA, as appears in the expression

$$G_{np} = \gamma \mathrm{ASA} + b \qquad (3)$$

The pore region was excluded from these calculations since it is occupied by water molecules, when gramicidin is both in the aqueous phase and in the lipid bilayer. We used the parameters $\gamma = 0.0278$ kcal/(mol Å^2) and $b = -1.71$ kcal/mol that have been derived from the partitioning of alkanes between liquid alkanes and water (*59*) and have been successfully used in our previous studies. The total area of gramicidin accessible to lipids in a particular configuration was calculated with a modified Shrake−Rupley (*62*) algorithm.

Gramicidin Structures. Three NMR PDB entries and one X-ray crystal PDB entry of gramicidin were tested: 1GRM (*61*; 5 NMR conformations), 1MAG (*15*; one NMR conformation), 1MIC (*63*; 20 NMR conformations), and 1AV2 (*16*; an X-ray structure). In the first two entries, gramicidin is a head-to-head dimer of two single-stranded (SS) β-helices (e.g., Figures 1 and 2), and in the last two it is a double-stranded (DS) intertwined dimer. In contrast to the other three entries, the 1MIC structure is closed; i.e., it does not form a pore and therefore does not represent an ion-conducting channel.

We added hydrogen atoms to the structures where they were missing and energy-minimized the new structure (100 steps of steepest descent), using the DISCOVER module of the Insight-II program (MSI, San Diego, CA).

Conformational Effects on the Transfer Free Energy. Gramicidin is very sensitive to the external medium and may change its conformation in the transfer between different milieux. The stability of short polyalanine-like α-helices in aqueous solutions has been the subject of theoretical and experimental studies (e.g., refs *64*−*67*). These studies indicate that a complete helix-to-coil transition of a polyalanine helix of about 15 residues involves a close-to-zero free energy value. By extrapolation, the free energy change resulting from conformational changes during the membrane association of gramicidin (ΔG_{con} in eq 1) should be insignificant and was thus neglected. This issue is considered in the Error Estimate section below.

Gramicidin Immobilization. Each gramicidin molecule has six external degrees of freedom, three translational and three rotational, and is free to translate and rotate when it is in bulk solution. Upon insertion into the membrane, the molecule can move only conjunct to the membrane, thus retaining only two free translational degrees of freedom and one free rotational degree of freedom. The other external degrees of freedom are partially lost and give rise to the free energy penalty of immobilization, ΔG_{imm}. An upper-bound estimate for the total immobilization free energy loss involved in the membrane insertion of polyalanine α-helices has been calculated as ∼3.7 kcal/mol (*68*). This estimate was also used for gramicidin because of the similarity between the two systems. The value of ΔG_{imm} weakly depends on the contact area between the peptide and the bilayer, and the above estimate is for a bilayer of native width. Our calculations show that gramicidin insertion into the bilayer involves local thinning of the membrane (see Results below) and hence leads to a decrease in the contact area between gramicidin and the membrane. Thus, the actual value of ΔG_{imm} is probably slightly lower.

Lipid Perturbation Effects. The insertion of hydrophobic intrusion into the bilayer interferes with it and gives rise to the lipid perturbation effect. The entropic nature of the effect implies that the lipid perturbation free energy, ΔG_{lip}, is proportional to the contact area between the peptide and the lipid molecules. Statistical thermodynamic calculations, based on a molecular model of the lipid chains, have provided an upper-bound estimate of $\Delta G_{lip} = 2.3$ kcal/mol for the insertion of polyalanine α-helices of hydrophobic length of approximately 30 Å (*44*, *68*). Since the hydrophobic length of gramicidin is approximately 22 Å (Figure 1), the contact area of gramicidin with the lipid membrane should be smaller than for polyalanine α-helices, and ΔG_{lip} is expected to be smaller than 2.3 kcal/mol. Nevertheless, we used the same upper-bound estimate in the calculations.

Membrane Deformation. Figure 1 shows that the hydrophobic core of gramicidin is a cylinder of approximate length 22 Å (see ref *2*), which is shorter than the 30 Å width of the hydrocarbon region of a native lipid bilayer. Thus, the insertion of gramicidin into a lipid bilayer may result in a deformation of the latter to match the hydrophobic length of the peptide, following the "mattress model" (*69*). The deformation involves a free energy penalty, ΔG_{def}, resulting from the compression of the lipid chains. ΔG_{def} has been calculated by several research groups using different methods, yielding similar values (e.g., refs *44* and *68*−*73*). We

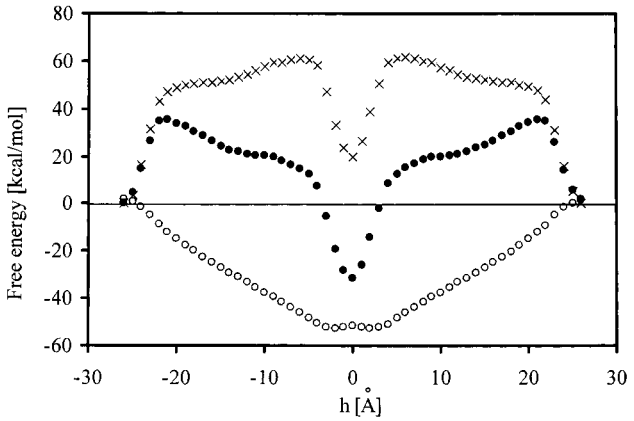

FIGURE 3: Vertical insertion of gramicidin into a bilayer along the hypothetical path of Figure 2A. ΔG_{np} (open circles), ΔG_{elc} (crosses), and ΔG_{sol} (full circles) as a function of the distance, h, between the geometrical center of gramicidin and the membrane midplane. The head-to-head homodimer 1GRM_1 structure was used, and the width of the hydrocarbon region of the membrane was set to 22 Å. The zero energy of the system was set to a configuration at which gramicidin is entirely in the aqueous phase (i.e., infinite gramicidin−membrane distance), and the calculations were carried out using a grid size of 129^3, a scale of three grid points per angstrom, and a pore dielectric constant of 10.

rely on the calculations of Fattal and Ben-Shaul (*44*) that are based on a statistical−thermodynamic molecular model of the lipid chains. A polynomial fit to these calculations gives

$$\Delta G_{def} = 0.0327 d_L^2 - 1.9342 d_L + 28.581 \qquad (4)$$

where ΔG_{def} is measured in kilocalories per mole and d_L is the width of the hydrocarbon region of the lipid bilayer, measured in angstroms.

RESULTS

A substantial amount of experimental data, referred to in the Discussion below, suggests that assembly of the gramicidin channel begins with monomer insertion at opposite sides, followed by dimerization. Yet, in this study we considered the insertion of gramicidin dimers into the lipid bilayer along two hypothetical paths: a vertical path, with the gramicidin principal axis perpendicular to the membrane surface (Figure 2A), and a horizontal one, with the gramicidin principal axis parallel to the membrane surface (Figure 2B). The first NMR structure from 1GRM, referred to as 1GRM_1, was used for most of the calculations because it exhibits the most negative free energy of transfer from the aqueous phase into the bilayer (see below).

Vertical Insertion. Figure 3 shows electrostatic, nonpolar, and solvation contributions to the free energy of transfer of gramicidin from water into a model lipid bilayer of hydrocarbon width of 22 Å as a function of the distance, h, between the geometrical center of gramicidin and the membrane midplane. The figure is roughly symmetrical around $h = 0$, where gramicidin is fully inserted into the membrane with its geometrical center in the bilayer midplane.

The insertion process may start either at $h = -26$ Å or at $h = +26$ Å, where one of gramicidin's C-termini is just in contact with the membrane surface. The nonpolar interactions drive the process. Their contribution is proportional to the surface area of gramicidin that is buried in the membrane, so that it changes in a roughly linear way with h, between $h = -26$ Å and $h = -4$ Å and between $h = +4$ Å and $h = +26$ Å. The interactions are saturated for $h = -4$ Å to $h = +4$ Å, before gramicidin begins to protrude again into the water at the other face of the membrane.

The electrostatic contribution depends on the polarity of the inserted part and thus increases sharply upon insertion of the polar indole side chains of the four tryptophan residues at the C-terminal half of the peptide (Figure 2) into the membrane ($h = -26$ Å to $h = -20$ Å and $h = +26$ Å to $h = +20$ Å). The steepness of the electrostatic free energy curve becomes moderate once the C-terminal region is fully buried in the bilayer, at $h = -20$ Å and $h = +20$ Å. At $h = -4$ Å and $h = +4$ Å, where the other polar C-terminal region protrudes into the aqueous phase from the opposite side of the membrane, there is a sharp decrease in the electrostatic free energy penalty. The minimal electrostatic free energy penalty was obtained at $h = 0$, where the C-terminal regions protrude evenly from both ends of the membrane.

The solvation free energy is the sum of the electrostatic penalty and nonpolar contributions (eq 2). Figure 3 shows that it is highly negative at the optimal location of $h = 0$, implying that gramicidin is likely to partition into the lipid bilayer. However, membrane association involves crossing a barrier of about 35 kcal/mol, due to the electrostatic penalty of removing the polar C-terminal region of one gramicidin monomer from the aqueous phase into the hydrocarbon region of the bilayer. It is obvious from the barrier height that gramicidin insertion into the bilayer cannot proceed along the path of Figure 3. This issue is discussed below.

The most favorable location of gramicidin in the membrane is obtained at $h = 0$, where the solvation free energy reaches its most negative value of −32 kcal/mol. In this gramicidin−membrane configuration the two C-terminal regions protrude into the aqueous phase and the electrostatic free energy penalty is minimal. Such a configuration is possible only if the length of the hydrophobic core of gramicidin matches the width of the hydrocarbon region of the bilayer, i.e., if the membrane is locally distorted.

Membrane Width. The native width of the hydrocarbon region of biological membranes is about 30 Å, while the hydrophobic core of gramicidin is only 22 Å long (Figure 1; ref *2*). Thus, insertion of gramicidin into bilayers of native width involves burial of gramicidin's C-terminal regions inside the bilayer, which results in a large electrostatic free energy penalty (Figure 3). The alternative involves membrane deformation to match the length of the hydrophobic core of gramicidin. We carried out a series of calculations of the insertion free energy of gramicidin into lipid bilayers of different widths to test this possibility. Table 1 and Figure 4 summarize the results of the calculations and enable the estimation of the most favorable membrane width. The table shows that membrane thinning has an opposing effect on ΔG_{sol} and ΔG_{def}; the former decreases (becomes more negative) while the latter increases with the decrease of the membrane width. This balance determines the most favorable membrane width for gramicidin insertion, which is associated with the most negative value of ΔG_{tot} and which was observed at 22 Å. This width was found to be the most favorable one for all of the conformations in PDB entry

Table 1: Effects of Insertion of Gramicidin into a Lipid Bilayer on the Membrane Curvature

membrane width[a] (Å)	ΔG values (kcal/mol)						
	ΔG_{np}[b]	ΔG_{elc}[c]	ΔG_{sol}[d]	ΔG_{imm}[e]	ΔG_{lip}[f]	ΔG_{def}[g]	ΔG_{tot}[h]
21	−48.1	17.1	−31.1	3.7	2.3	2.4	−23
22	−51.4	19.7	−31.7	3.7	2.3	1.9	−24
23	−55.7	26.0	−29.7	3.7	2.3	1.4	−22
24	−59.3	34.6	−24.8	3.7	2.3	1.0	−18
30	−72.5	106.4	33.9	3.7	2.3	0.0	40

[a] The (local) width of the hydrocarbon region of the bilayer. [b] The nonpolar contribution to the solvation free energy. [c] The electrostatic contribution to the solvation free energy. [d] The solvation free energy. [e] The peptide immobilization free energy. [f] The lipid perturbation free energy. [g] The membrane deformation free energy. [h] The total free energy (eq 1). The 1GRM_1 structure was used, and the values reported were calculated at the most favorable location, $h = 0$. The calculations were carried out with a cubic grid of 129^3 points, a scale of three grid points per angstrom, and a pore dielectric constant of 10.

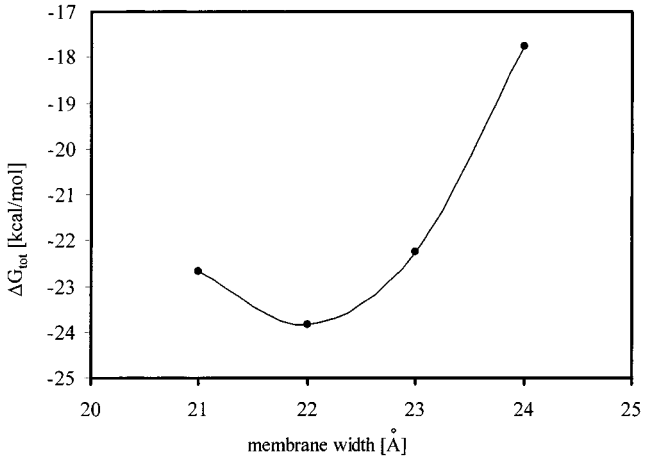

FIGURE 4: ΔG_{tot} dependence on the (local) width of the hydrocarbon region of the bilayer (values taken from Table 1). The most negative value of ΔG_{tot} was obtained at a membrane width of 22 Å.

1GRM and for most of the gramicidin structures that were tested (see below). We therefore used it for the remainder of calculations, unless otherwise stated.

Conformations. A total of 27 gramicidin conformations of four different PDB entries were tested. Of the four entries, two are single-stranded (SS) head-to-head dimers [PDB identifiers: 1GRM (5 conformers) and 1MAG (1 conformer)] and two are double-stranded (DS) intertwined dimers [PDB identifiers 1MIC (20 conformers) and 1AV2 (one conformer)]. We repeated the calculations of Figure 3 for all of these conformations. That is, we calculated the free energy of transfer of gramicidin in each of the 27 conformations from the aqueous phase into lipid bilayers of different width at different locations. The results of these calculations are summarized in Table 2, which presents the most negative value of the transfer free energy obtained for each PDB entry and the membrane width at which it was obtained. It also presents the free energy breakdown. It is evident from the table that, while gramicidin may partition into the membrane in all of the conformations that were tested, the most negative value of the transfer free energy was obtained for the single-stranded head-to-head β-helix dimer of 1GRM_1. This value is significantly more negative than the values obtained for the other conformations, suggesting that 1GRM_1 is the most likely conformation of gramicidin in lipid bilayers. We

Table 2: Effects of Gramicidin Conformation on the Free Energy of Membrane Insertion

PDB entry[a]	membrane width[b] (Å)	ΔG values (kcal/mol)						
		ΔG_{np}[c]	ΔG_{elc}[d]	ΔG_{sol}[e]	ΔG_{imm}[f]	ΔG_{lip}[g]	ΔG_{def}[h]	ΔG_{tot}[i]
1GRM_1	22	−51.4	19.7	−31.7	3.7	2.3	1.9	−24
1MAG	21	−49.1	21.9	−27.2	3.7	2.3	2.4	−19
1MIC_2	21	−49.0	26.6	−22.4	3.7	2.3	2.4	−14
1AV2	20	−47.7	35.5	−12.2	3.7	2.3	3.0	−3

[a] The PDB identifier of the gramicidin structure used. In cases where multiple NMR conformations are given, the most negative value of ΔG_{tot} is reported, and the extra number following the underscore indicates the conformer number in the PDB entry. [b] The width of the hydrocarbon region of the bilayer associated with the most negative value of ΔG_{tot}. [c] The nonpolar contribution to the solvation free energy. [d] The electrostatic contribution to the solvation free energy. [e] The solvation free energy. [f] The peptide immobilization free energy. [g] The lipid perturbation free energy. [h] The membrane deformation free energy. [i] The total free energy (eq 1). The calculations were carried out with a cubic grid of 129^3 points, a scale of three grid points per angstrom, and a pore dielectric constant of 10.

therefore used it throughout this study. It is noteworthy that, regardless of the conformation, gramicidin insertion into lipid bilayers is likely to involve a significant local thinning of the membrane.

Our calculations also demonstrate that relatively minor structural changes can affect the value of ΔG_{sol}, and therefore ΔG_{tot}, significantly; differences as high as 7 kcal/mol were obtained between NMR conformers of the same PDB entry with trace root mean square deviations (RMSD) of less than 0.7 Å. These differences usually reflected variations in the configuration of backbone hydrogen bonds. The dipoles of the N−H and C═O groups neutralize each other to a large extent in the vicinity of the optimal hydrogen-bonding configuration, such that the free energy of transfer of an optimal backbone hydrogen bond from the aqueous phase into the hydrocarbon region of the bilayer (ΔG_{sol}) is only about 2 kcal/mol (*45*). Slight changes in the distance between the hydrogen donor and acceptor or in the inclination angle between the N−H and C═O groups typically disrupt the degree of neutralization and therefore involve an increase in the magnitude of the ΔG_{sol} penalty.

In view of this, the ∼5 kcal/mol difference in the ΔG_{sol} values of the 1GRM_1 and 1MAG structures (Table 2) is not surprising. Even though both are single-stranded head-to-head dimers of the same fold, their trace RMSD is ∼1.2 Å. In fact, the 1GRM_1 structure is elongated, and its hydrophobic region is ∼1 Å longer than that of 1MAG. Thus, its transfer from the aqueous phase into the membrane involves a reduced membrane thinning compared to that of 1MAG. This obviously leads to a 0.5 kcal/mol decrease in the magnitude of the ΔG_{def} penalty of 1GRM_1 compared to 1MAG. Moreover, it leads to an increase of 2.3 kcal/mol in the magnitude of the nonpolar contribution to ΔG_{sol} in 1GRM_1 compared to 1MAG because of the increase in the area of the gramicidin−membrane interface. The rest of the ∼5 kcal/mol difference is mainly due to accumulative effects of slight changes in the electrostatic desolvation penalty associated with the transfer of backbone hydrogen bonds from the aqueous phase into the hydrocarbon region of the bilayer.

Horizontal Insertion. The ion-conducting state of gramicidin exists when it is vertically inserted into the lipid bilayer

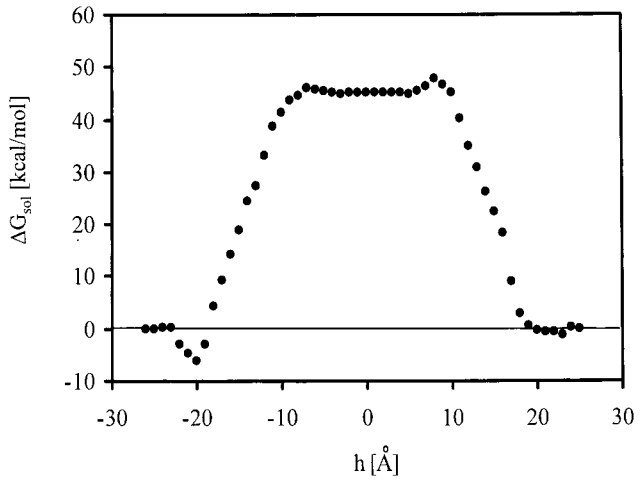

FIGURE 5: Horizontal insertion of gramicidin into a bilayer along the hypothetical path of Figure 2B. ΔG_{sol} as a function of the distance, *h*, between the geometrical center of gramicidin and the membrane midplane. The 1GRM_1 structure was used, and the width of the hydrocarbon region of the membrane was set to its native value of 30 Å. The zero free energy of the system was set to a configuration at which gramicidin is entirely in the aqueous phase (i.e., infinite gramicidin−membrane distance), and the calculations were carried out using a grid size of 129^3, a scale of three grid points per angstrom, and a pore dielectric constant of 10. The solvation free energy minimum of about −6 kcal/mol can be seen at $h = -20$ Å, where gramicidin is horizontally adsorbed on the surface of the bilayer.

(Figure 3, $h = 0$). Nevertheless, other membrane-associated orientations may be energetically favorable and may serve as intermediates in the insertion process. We tested several orientations, and Figure 5 presents data obtained for insertion of 1GRM_1 into the membrane along the hypothetical horizontal path of Figure 2B. The solvation free energy curve obtained for horizontal insertion is significantly different from the curve obtained for vertical insertion (Figure 3, filled circles). It is characterized by a moderate minimum, at $h = -20$ Å, where the hydrophobic side chains are inserted into the bilayer while the polar terminal regions are still in the aqueous phase, and by a high flat maximum, between $h = -8$ Å and $h = 10$ Å, where the terminal regions are fully buried in the bilayer.

Convergence Tests. All of the calculations were carried out using a grid of 129^3 points and a scale of three grid points per angstrom. We repeated the calculations (with the 1GRM_1 structure) using a grid size of 161^3 and scales of four and five grid points per angstrom to test the convergence of the calculations. The results indicate that the calculations converged to less than 0.3 kcal/mol. This high precision is a result of the simple model that we used to characterize the system, e.g., the neglect of the polar headgroup region of the bilayer and the conformational freedom of gramicidin. These simplifications of the model may result in higher systematic errors, as discussed below.

ERROR ESTIMATE

The limitations of the continuum solvent model, and in particular the slab representation of the bilayer, for the treatment of peptide−membrane systems, have been discussed at length (*43*, *45*, *51*−*54*, *74*−*76*). The main shortcoming of the model is the neglect of the polar headgroup region. However, accumulative evidence (reviewed in ref *46*) suggests that this should not be a major problem for highly hydrophobic peptides such as gramicidin, which interact predominantly with the hydrocarbon region of the bilayer (*2*).

The main uncertainty in continuum solvent treatment of the gramicidin channel is the value assigned to the dielectric constant inside the pore. The choice of this value is crucial in studies of the channel conductivity (e.g., refs *34*−*36* and *77*). However, our calculations demonstrate that the solvation free energy is, in essence, independent of the value assigned to the dielectric constant inside the pore. We repeated the calculations of Figure 3 using several values of the pore dielectric constant in the range 2−80. The calculations showed that the variance between the solvation free energy values was only 0.1 kcal/mol at $h = 0$, in the most stable gramicidin−bilayer configuration (data not shown).

While the solvation contributions to the transfer free energy were explicitly calculated, the values assigned to the other terms in eq 1 are based on estimates. The main source of error in this study probably derives from these terms. Three of these terms are related to the structure and elasticity of the membrane: the free energy penalties associated with the effects of gramicidin immobilization, lipid perturbation, and membrane deformation. All together these estimates give a penalty of about 8−9 kcal/mol, which is an upper bound to the correct value as indicated in Methods above. It is important to emphasize that these values depend on the contact area between gramicidin and the bilayer. The latter varies very little between the different gramicidin structures used in this study. Thus, differences in the total free energy of transfer of these structures from the aqueous phase into the bilayer ($\Delta\Delta G$) are probably much more accurate than the transfer free energies of individual structures.

An important concern in this study is the assumption that gramicidin was taken as a rigid body in all sets of calculations. In fact, structure flexibility was taken into account to some extent by carrying out sets of calculations using the 27 experimentally observed structures (as opposed to the use of only one structure).

The main uncertainty in this study comes from the estimate of ΔG_{con}, the free energy difference due to conformational changes in the structure of gramicidin in the transfer from the aqueous phase into the bilayer. Since it is virtually impossible to measure or calculate this value directly, we had to use an alternative. Our approach was based on a hypothetical path, according to which gramicidin assumes its membrane-associated conformation in the aqueous phase prior to its insertion into the lipid bilayer. The underlying assumption here was that at least 1 of the 27 experimentally determined structures that we used approximates the correct structure of the peptide in the membrane. While this assumption is common in most of the continuum solvent model and molecular dynamics studies, it needs to be experimentally verified.

Following this approach, the ΔG_{con} contribution should be estimated for virtual structural changes that occur at the aqueous phase. The highly hydrophobic nature of gramicidin precludes direct measurement of such changes, and the unique structural features of gramicidin, e.g., the facts that its sequence includes both L- and D-amino acids and that it forms β-helices, make it very difficult to calculate the ΔG_{con} contribution directly. Thus, we were forced to rely on estimates derived from studies on related systems and

assumed that the value of ΔG_{con} should be approximately 0 (see Methods above). This assumption is consistent with the fact that gramicidin was experimentally detected in a variety of conformations; had ΔG_{con} been significantly larger, only one conformation would have been observed.

Recent experimental and theoretical−computational studies of folding and stability in soluble peptides of up to 30−40 residues that adapt α and β structures indicate that the folding free energy usually does not exceed 5 kcal/mol (*66*, *67*, *78*−*87*). This value can be regarded as an upper bound to the free energy change resulting from conformational changes during the membrane association of gramicidin (ΔG_{con}).

Again, for the current study, differences in the value of the ΔG_{con} component between the various gramicidin structures ($\Delta\Delta G_{con}$) are more important than absolute values of ΔG_{con} associated with conformational changes of each structure. These differences should be much smaller than 5 kcal/mol, since gramicidin shifts between well-defined conformations, rather than undergoing a complete unfolding. In summary, while the ΔG_{tot} values of Table 2 should be regarded as estimates with about ±5 kcal/mol accuracy, differences between them ($\Delta\Delta G_{tot}$) should be significantly more accurate with a maximum error of ±3 kcal/mol.

DISCUSSION

Gramicidin is very hydrophobic and our calculations have shown that it is likely to partition into lipid bilayers in all of the conformations that were tested, both as a head-to-head dimer of two single-stranded (SS) helices and as an intertwined double-stranded (DS) helix, in open (ion-conducting) and closed conformations (Table 2). Interestingly, of the two DS conformations, 1MIC (*63*), which is closed and cannot serve as a channel, was found to be very stable in membranes. In contrast, the 1AV2 (*16*) conformation, which has a pore and may be capable of conducting ions, was found to be only marginally stable in the bilayer. One obvious conclusion from the calculations is that the SS conformations [PDB identifiers: 1GRM (*61*) and 1MAG (*15*)] are significantly more stable than the DS conformations [PDB identifiers: 1MIC (*63*) and 1AV2 (*16*)] in bilayers (Table 2). This is mainly due to the four Trp residues of gramicidin (*19*, *88*). Membrane insertion of the DS structures involves burying these residues inside the hydrocarbon region of the bilayer. This leads to a large electrostatic free energy penalty, mainly due to the transfer of the polar N−H groups of the Trp side chains from the polar phase, where they can form hydrogen bonds with water molecules or the polar headgroups, into the hydrocarbon region of the bilayer, which has no hydrogen-bonding capabilities. In contrast, in the SS structures, the Trp residues are located close to each other at the C-terminus of each monomer (Figure 2), and the membrane may deform to avoid this penalty (Figure 6).

The calculations showed that of the six SS conformations (five in 1GRM and one in 1MAG), 1GRM_1 is associated with the most negative ΔG_{tot} value, thus supporting the previous view that it is the main conformation of the channel in membranes. The fact that both the SS and DS conformations were found to be stable in the membrane may explain why both were experimentally detected. The calculations have shown that while gramicidin may associate with bilayers

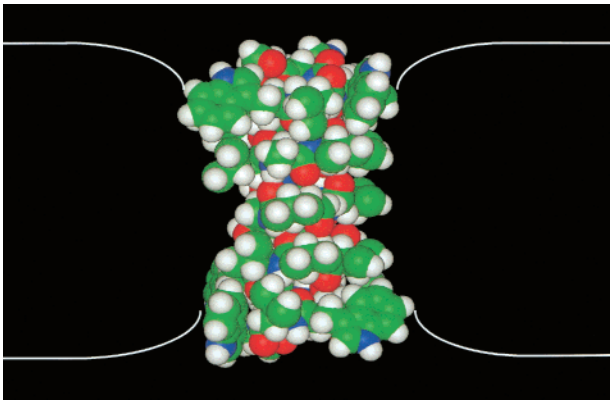

FIGURE 6: Schematic representation of gramicidin in the locally deformed lipid bilayer. The space-filling model of the peptide (1GRM_1) was displayed with INSIGHT-II (MSI, San Diego, CA). Oxygen atoms are in red, carbon atoms are in green, nitrogen atoms are in blue, and hydrogen atoms are in white. The two white lines represent the boundaries of the hydrocarbon region of the lipid bilayer.

in a surface orientation (Figure 5; $\Delta G_{tot} \sim -6$ kcal/mol), it is much more stable in a transmembrane orientation (Figure 3; $\Delta G_{tot} \sim -24$ kcal/mol). This is to be expected, given its role as a channel, and is in accordance with the experimental data (e.g., ref *2*). The ΔG_{tot} value obtained for the transmembrane orientation is very negative, suggesting that gramicidin will be predominantly in this orientation and will, in essence, be excluded from the aqueous phase.

The hydrophobic length of the gramicidin dimer is shorter than the width of the hydrocarbon region of the native bilayer, and the calculations have demonstrated that, regardless of the conformation of gramicidin, its membrane insertion is likely to involve a significant local thinning. In particular, membrane insertion of the channel in its most stable conformation, 1GRM_1, is likely to involve local membrane deformation to match the 22 Å length of 1GRM_1 (Figure 6). This is in very high conformity with the available experimental data (*2*, *22*−*27*) and the vast majority of theoretical−computational work (e.g., refs *28*−*32*). However, it is in conflict with recent molecular dynamics (MD) simulations (*33*). A possible explanation for the discrepancy between the MD simulations and the rest of the studies (including this one) is that the electrostatic free energy penalty associated with the transfer of the polar C-termini of the gramicidin channel from the aqueous phase into the hydrocarbon region of the bilayer may have not been fully taken into account. Other possibilities are discussed in the original paper (*33*).

Membrane insertion of two antimicrobial peptides, gramicidin and alamethicin (*51*, *89*), involves local membrane deformation. One possible reason that comes to mind is that since both peptides are designed to make the membrane permeable, evolutionary pressure has led to the design of the most economical peptides, which are just long enough to span the membrane, to minimize the energetic cost of their synthesis. Thus, alamethicin, which is the less hydrophobic of the two, can only induce a minor deformation of about 2 Å, while gramicidin can significantly deform the membrane.

Figure 3 shows that membrane insertion of 1GRM_1, the most stable form of gramicidin in the bilayer, involves crossing a free energy barrier of about 35 kcal/mol. Similar calculations, carried out using the other structures, have

shown that their membrane insertion also involves crossing large free energy barriers; the smallest barriers (about 23 kcal/mol) were obtained for the 1MAG and 1MIC structures (data not shown). Evidently, therefore, the insertion path of Figure 3 is unrealistic. There are no data on the path taken for gramicidin insertion into membranes in vivo. However, all of the available in vitro kinetic measurements support the notion that the monomers are first inserted at opposite ends and subsequently, due to fluctuations in the thickness of the membrane, dimerize to form a conducting channel (*23*−*26*, *90*; reviewed in ref *2*).

REFERENCES

1. Andersen, O. S. (1984) *Annu. Rev. Physiol. 46*, 531−548.
2. Killian, J. A. (1992) *Biochim. Biophys. Acta 1113*, 391−425.
3. Roux, B., and Karplus, M. (1994) *Annu. Rev. Biophys. Biomol. Struct. 23*, 731−761.
4. Wallace, B. A. (2000) *BioEssays 22*, 227−234.
5. Sarges, R., and Witkop, B. (1965) *J. Am. Chem. Soc. 87*, 2011−2020.
6. Urry, D. W. (1971) *Proc. Natl. Acad. Sci. U.S.A. 68*, 672−667.
7. Urry, D. W. (1972) *Proc. Natl. Acad. Sci. U.S.A. 69*, 1610−1614.
8. Veatch, W. R., Fossel, E. T., and Blour, E. R. (1974) *Biochemistry 13*, 5249−5256.
9. Urry, D. W., Goodall, M. C., Glickson, J. D., and Mayers, D. F. (1971) *Proc. Natl. Acad. Sci. U.S.A. 68*, 1907−1911.
10. Ramachandran, G. N., and Chandrasekaran, R. (1972) *Ind. J. Biochem. Biophys. 9*, 1−11.
11. Arsen'ev, A. S., Barsukov, I. L., Bystrov, V. F., Lomize, A. L., and Ovchinnikov, Y. A. (1985) *FEBS Lett. 186*, 168−174.
12. Nicholson, L. K., and Cross, T. A. (1989) *Biochemistry 28*, 9379−9385.
13. Koeppe, R. E., II, Providence, L. L., Greathouse, D. V., Heitz, F., Trudelle, Y., Purdie, N., and Andersen, O. S. (1992) *Proteins 12*, 49−62.
14. Busath, D. D. (1993) *Annu. Rev. Physiol. 55*, 473−501.
15. Ketchem, R. R., Lee, K. C., Huo, S., and Cross, T. A. (1996) *J. Biomol. NMR 8*, 1−14.
16. Burkhart, B. M., Li, N., Langs, D. A., Pangborn, W. A., and Duax, W. L. (1998) *Proc. Natl. Acad. Sci. U.S.A. 95*, 12950−12955.
17. Editorial (1998) *Nat. Struct. Biol. 5*, 749−750.
18. Andersen, O. S., Apell, H. J., Bamberg, E., Busath, D. D., Koeppe, R. E., II, Sigworth, F. J., Szabo, G., Urry, D. W., and Woolley, A. (1999) *Nat. Struct. Biol. 6*, 609.
19. Cross, T. A., Arseniev, A., Cornell, B. A., Davis, J. H., Killian, J. A., Koeppe, R. E., II, Nicholson, L. K., Separovic, F., and Wallace, B. A. (1999) *Nat. Struct. Biol. 6*, 610−611.
20. Burkhart, B. M., and Duax, W. L. (1999) *Nat. Struct. Biol. 6*, 611−612.
21. White, S. H., and Wimley, W. C. (1999) *Annu. Rev. Biophys. Biomol. Struct. 28*, 319−365.
22. Bamberg, E., and Benz, R. (1976) *Biochim. Biophys. Acta 426*, 570−580.
23. Kolb, H. A., and Bamberg, E. (1977) *Biochim. Biophys. Acta 464*, 127−141.
24. Elliott, J. R., Needham, D., Dilger, J. P., and Haydon, D. A. (1983) *Biochim. Biophys. Acta 735*, 95−103.
25. O'Connell, A. M., Koeppe, R. E., II, and Andersen, O. S. (1990) *Science 250*, 1256−1259.
26. Durkin, J. T., Providence, L. L., Koeppe, R. E., II, and Andersen, O. S. (1993) *J. Mol. Biol. 231*, 1102−1121.
27. Harroun, T. A., Heller, W. T., Weiss, T. M., Yang, L., and Huang, H. W. (1999) *Biophys. J. 76*, 937−945.
28. Ring, A. (1996) *Biochim. Biophys. Acta 1278*, 147−159.
29. Lundbaek, J. A., and Andersen, O. S. (1999) *Biophys. J. 76*, 889−895.
30. Harroun, T. A., Heller, W. T., Weiss, T. M., Yang, L., and Huang, H. W. (1999) *Biophys. J. 76*, 3176−3185.
31. Huang, H. W. (1999) *Novartis Found. Symp. 225*, 188−200.
32. May, S. (2000) *Eur. Biophys. J. 29*, 17−28.
33. Chiu, S. W., Subramaniam, S., and Jakobsson, E. (1999) *Biophys. J. 76*, 1929−1938.
34. Chiu, S. W., Subramaniam, S., and Jakobsson, E. (1999) *Biophys. J. 76*, 1939−1950.
35. Roux, B. (1999) *Biophys. J. 77*, 139−153.
36. Cardenas, A. E., Coalson, R. D., and Kurnikova, M. G. (2000) *Biophys. J. 79*, 80−93.
37. Jakobsson, E. (1998) *Methods 14*, 342−351.
38. Sansom, M. S., Shrivastava, I. H., Ranatunga, K. M., and Smith, G. R. (2000) *Trends Biochem. Sci. 25*, 368−374.
39. Woolf, T. B., and Roux, B. (1996) *Proteins 24*, 92−114.
40. Engelman, D. M., and Steitz, T. A. (1981) *Cell 23*, 411−422.
41. Jähnig, F. (1983) *Proc. Natl. Acad. Sci. U.S.A. 80*, 3691−3695.
42. Jacobs, R. E., and White, S. H. (1989) *Biochemistry 28*, 3421−3437.
43. Milik, M., and Skolnick, J. (1993) *Protein 15*, 10−25.
44. Fattal, D. R., and Ben-Shaul, A. (1993) *Biophys. J. 65*, 1795−1809.
45. Ben-Tal, N., Ben-Shaul, A., Nichols, A., and Honig, B. (1996) *Biophys. J. 70*, 1803−1812.
46. Kessel, A., and Ben-Tal, N. (2002) in *Current Topics in Membranes: Peptide*−*Lipid Interactions* (Simon, S., and McIntosh, T., Eds.) Vol. 52, pp 205−253, Academic Press, San Diego.
47. Gilson, M. K. (1995) *Curr. Opin. Struct. Biol. 5*, 216−223.
48. Honig, B., and Nichols, A. (1995) *Science 268*, 1144−1149.
49. Nakamura, H. (1996) *Q. Rev. Biophys. 29*, 1−90.
50. Warshel, A., and Papazyan, A. (1998) *Curr. Opin. Struct. Biol. 8*, 211−217.
51. Kessel, A., Cafiso, D. S., and Ben-Tal, N. (2000) *Biophys. J. 78*, 571−583.
52. Kessel, A., Schulten, K., and Ben-Tal, N. (2000) *Biophys. J. 79*, 2322−2330.
53. Bechor, D., and Ben-Tal, N. (2001) *Biophys. J. 80*, 643−655.
54. Ben-Tal, N., Sitkoff, D., Bransburg-Zabary, S., Nachliel, E., and Gutman, M. (2000) *Biochim. Biophys. Acta 1466*, 221−233.
55. Kessel, A., Musafia, B., and Ben-Tal, N. (2001) *Biophys. J. 80*, 2536−2545.
56. Kessel, A., Ben-Tal, N., and May, S. (2001) *Biophys. J. 81*, 643−658.
57. Honig, B., Sharp, K., and Yang, A.-S. (1993) *J. Phys. Chem. 97*, 1101−1109.
58. Sitkoff, D., Sharp, K., and Honig, B. (1994) *J. Phys. Chem. 98*, 1978−1988.
59. Sitkoff, D., Ben-Tal, N., and Honig, B. (1996) *J. Phys. Chem. 100*, 2744−2752.
60. Sharp, K. A., Nicholls, A., Fine, R. M., and Honig, B. (1991) *Science 252*, 106−109.
61. Lomize, A. L., Orekhov, V. Iu., and Arsen'ev, A. S. (1992) *Bioorg. Khim. 18*, 182−200 (in Russian).
62. Shrake, A., and Rupley, J. A. (1973) *J. Mol. Biol. 79*, 351−371.
63. Chen, Y., Tucker, A., and Wallace, B. A. (1996) *J. Mol. Biol. 264*, 757−769.
64. Zimm, B. H., and Bragg, J. K. (1959) *J. Chem. Phys. 31*, 526−535.
65. Lifson, S., and Roig, A. (1961) *J. Chem. Phys. 34*, 1963−1974.
66. Scholtz, J. M., and Baldwin., R. L. (1992) *Annu. Rev. Biophys. Biomol. Struct. 21*, 95−118.
67. Chakrabartty, A., and Baldwin, R. L. (1995) *Adv. Protein Chem. 46*, 141−176.
68. Ben-Shaul, A., Ben-Tal, N., and Honig, B. (1996) *Biophys. J. 71*, 130−138.
69. Mouritsen, O. G., and Bloom, M. (1984) *Biophys. J. 46*, 141−153.

70. Helfrich, P., and Jakobsson, E. (1990) *Biophys. J. 57*, 1075−1084.
71. Nielsen, C., Goulian, M., and Andersen, O. S. (1998) *Biophys. J. 74*, 1966−1983.
72. Dan, N., and Safran, S. A. (1998) *Biophys. J. 75*, 1410−1414.
73. May, S., and Ben-Shaul, A. (1999) *Biophys. J. 76*, 751−767.
74. Berneche, S., Nina, M., and Roux, B. (1998) *Biophys. J. 75*, 1603−1618.
75. La Rocca, P., Shai, Y., and Sansom, M. S. (1999) *Biophys. Chem. 76*, 145−159.
76. Nina, M., Berneche, S., and Roux, B. (2000) *Eur. Biophys. J. 29*, 439−454.
77. Kurnikova, M. G., Coalson, R. D., Graf, P., and Nitzan, A. (1999) *Biophys. J. 76*, 642−656.
78. Wöjcik, J., Altmann, K. H., and Scheraga, H. A. (1990) *Biopolymers 30*, 121−134.
79. Boczko, E. M., and Brooks, C. L., III (1995) *Science 269*, 393−396.
80. Yang, A. S., and Honig, B. (1995) *J. Mol. Biol. 252*, 351−365.
81. Guerois, R., and Serrano, L. (2001) *Curr. Opin. Struct. Biol. 11*, 101−106.
82. Young, W. S., and Brooks, C. L., III (1996) *J. Mol. Biol. 259*, 560−572.
83. Guo, Z., Brooks, C. L., III, and Boczko, E. M. (1997) *Proc. Natl. Acad. Sci. U.S.A. 94*, 10161−10166.
84. Brooks, C. L., III (1998) *Curr. Opin. Struct. Biol. 8*, 222−226.
85. Bursulaya, B. D., and Brooks, C. L., III (2000) *J. Phys. Chem. B 104*, 12378−12383.
86. Ferrara, P., Apostolakis, J., and Caflisch, A. (2000) *J. Phys. Chem. B 104*, 5000−5010.
87. Levy, Y., Jortner, J., and Becker, O. M. (2001) *Proc. Natl. Acad. Sci. U.S.A. 98*, 2188−2193.
88. Killian, J. A., and von Heijne, G. (2000) *Trends Biochem. Sci. 25*, 429−434.
89. Barranger-Mathys, M., and Cafiso, D. S. (1996) *Biochemistry 35*, 498−505.
90. Sandblom, J., Galvanovskis, J., and Jilderos, B. (2001) *Biophys. J. 81*, 827−837.
91. Nicholls, A., Sharp, K. A., and Honig, B. (1991) *Proteins 11*, 281−286.

BI0120704